

Supplementary Data for

Effect of pseudouridylation on the structure and activity of the catalytically essential P6.1 hairpin in human telomerase RNA

Nak-Kyoon Kim¹, Carla A. Theimer^{1,#}, James R. Mitchell^{2,%},
Kathleen Collins², and Juli Feigon^{1,*}

¹Department of Chemistry and Biochemistry, University of California, Los Angeles, CA 90095,

²Department of Molecular and Cell Biology, University of California, Berkeley, CA 94720,

[#]Current address: Department of Chemistry, State University of New York, Albany, NY 12222,

[%]Current address: Department of Genetics and Complex Diseases, Harvard School of Public Health, Boston, MA 20115

*Corresponding author: feigon@mbi.ucla.edu

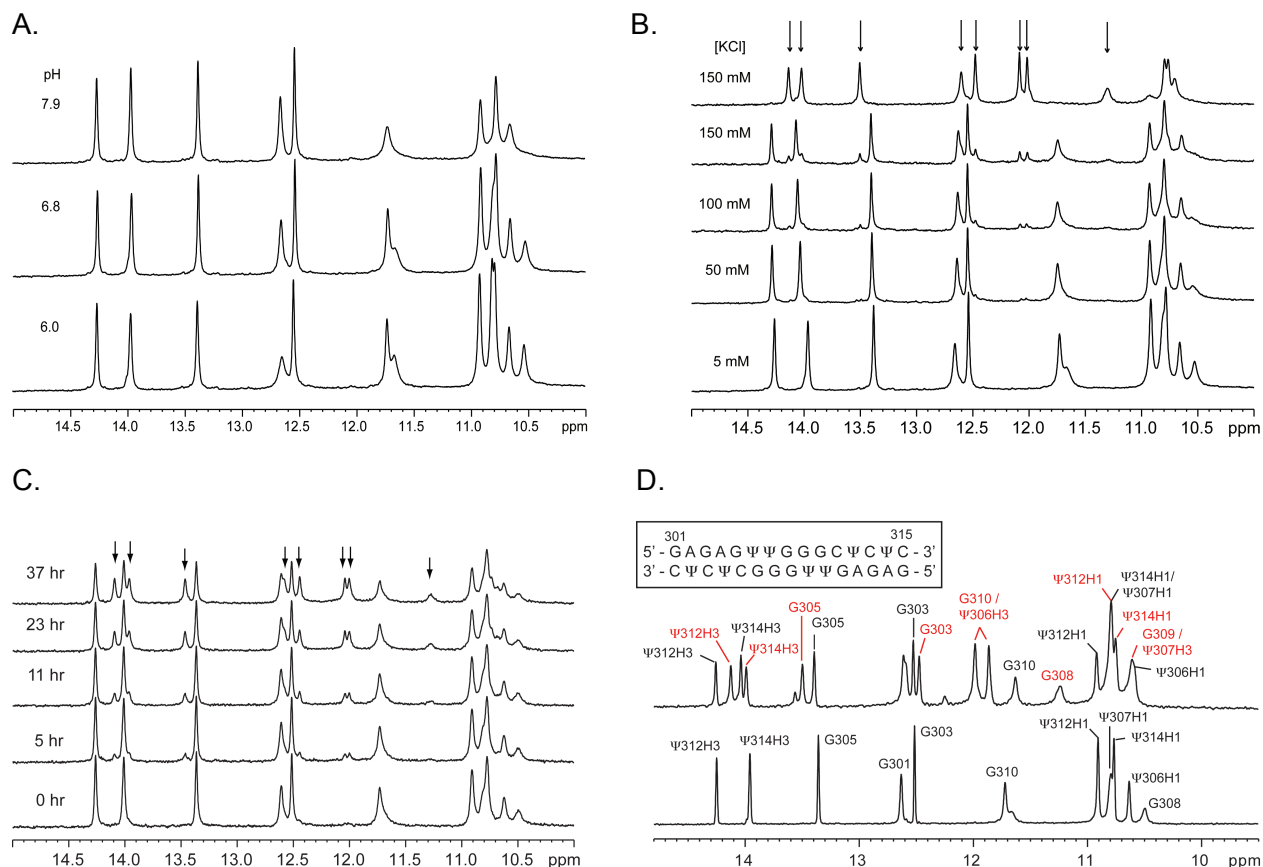


Figure S1. 1D imino proton spectra of Ψ4-P6.1 as a function of pH, salt, and time at 10°C. (A) pH dependence of sample in ~5 mM KCl. As pH is increased there is only a small effect on imino proton exchange for ΨH1s and G310H1, based on increasing line-width. (B) Effect of added KCl. As salt concentration is increased, the imino proton resonances of the hairpin do not shift significantly, indicating KCl does not affect the RNA structure. However as the salt increases, new resonances corresponding to the duplex appear. Spectra were taken within 15 minutes after addition of KCl. The RNA converts completely to duplex within 2 days (top spectrum). (C) Time dependence of appearance of duplex in the Ψ4-P6.1 sample after addition of 50 mM KCl. Sample is ~35% duplex after 37 hrs. Arrows in B and C point to imino proton resonances from duplex. (D) 1D imino spectra of Ψ4-P6.1 in conditions used for the structure determination (5 mM KCl, pH 6.8) [bottom] and sample in same conditions after storage at 20°C for about a week. Note that even at the low salt conditions of this study the sample converts partially to duplex over time, so samples were reannealed before and checked after each NMR experiment. Not all Ψ4-P6.1 become a duplex, but the hairpin and duplex become equilibrium (top). The duplex peaks are labeled in red, and the duplex sequence for Ψ4-P6.1 is shown in the box. Spectra were taken at 600 MHz for (A) and (B), 500 MHz for (C), and 800 MHz for (D).

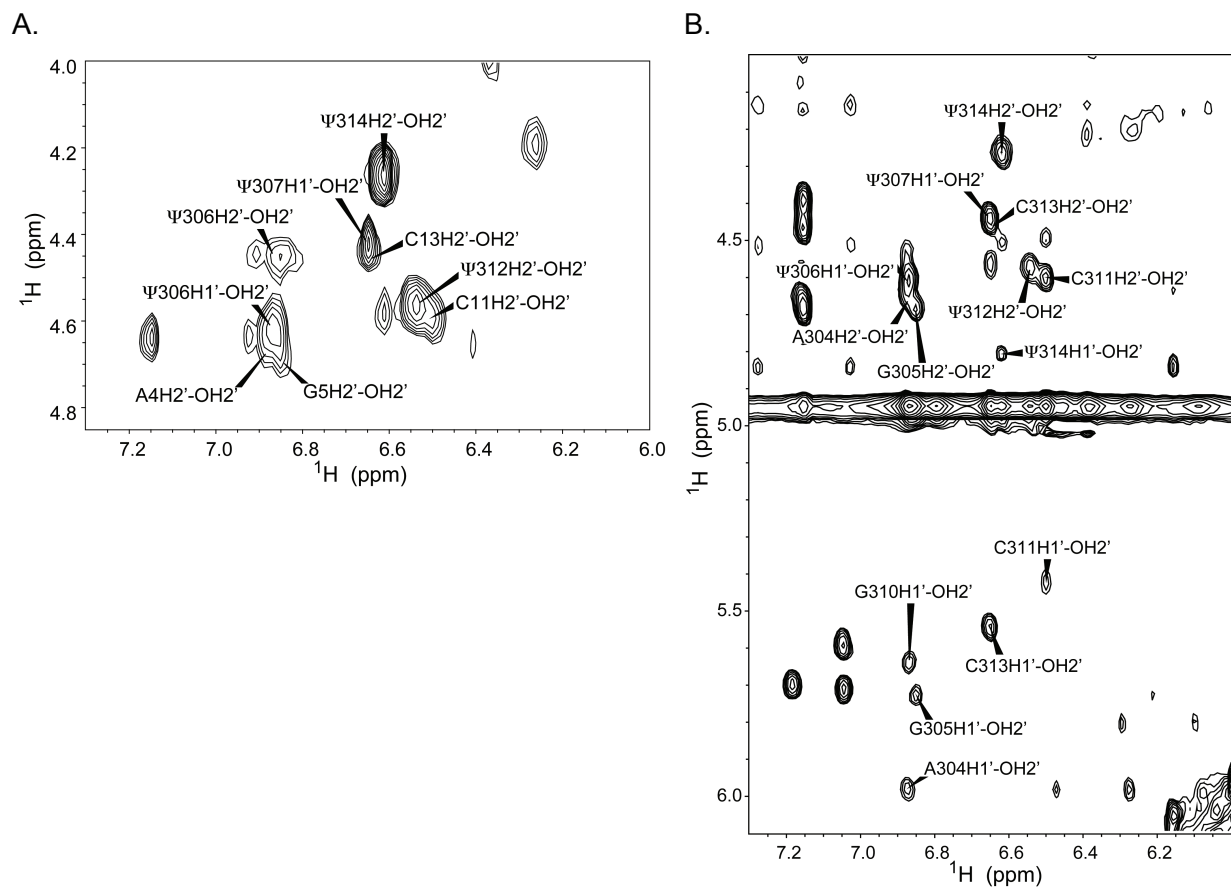


Figure S2. (A) 2D DIPSII TOCSY ($\tau_m=43\text{ms}$), and (B) 2D flip-back watergate NOESY ($\tau_m=50\text{ms}$) at 10°C and 800MHz . Assignments of some 2'-hydroxyl protons of $\Psi 4\text{-P6.1}$ RNA are labeled.

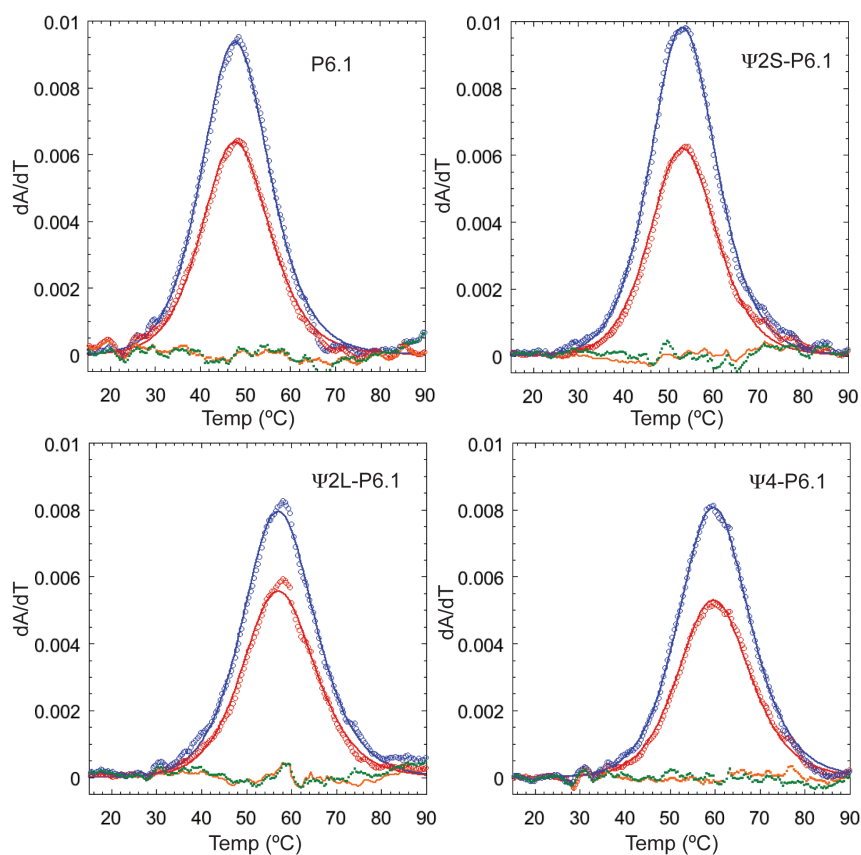


Figure S3. Representative 1st derivative plots (dA/dT) of UV thermal denaturation absorbance profile for P6.1 RNAs. Open circles are experimental data, and the calculated line fits to the experimental data are shown as solid lines. Absorbance was measured at two wavelengths (260 nm: blue and 280 nm: red), and the residuals (difference between experimental and calculated data) are shown in green for 260 nm measurements and orange for 280 nm.

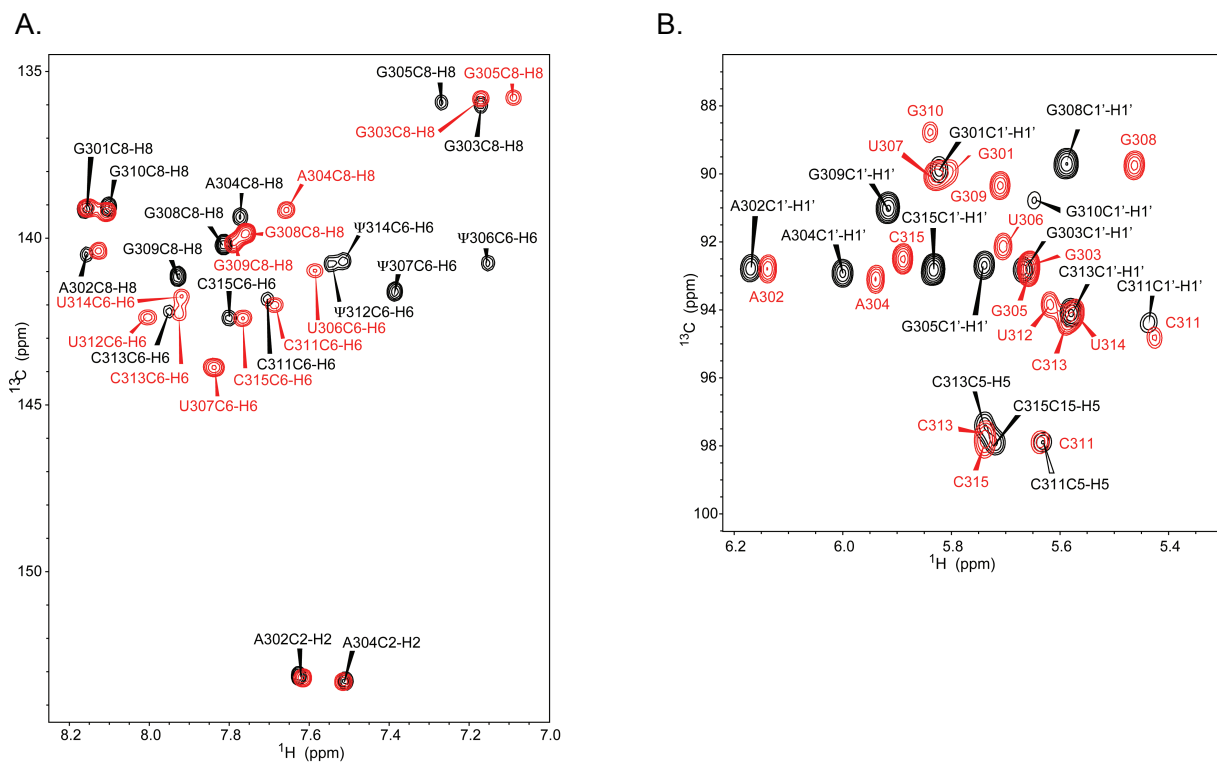


Figure S4. Comparison of (A) aromatic and (B) C1'-H1' and C5-H5 regions of 2D ^{13}C - ^1H HSQC NMR spectra (500MHz, 20°C) of Ψ 4-P6.1 (black) and P6.1 (red). Large chemical shift differences are observed for the residues 305, 308, 309, and 310 as well as for positions 306, 307, 312, and 314 (Ψ vs U). Cross peaks for Ψ C1'-H1' are not shown since they are upfield shifted into the C4'-H4' region.

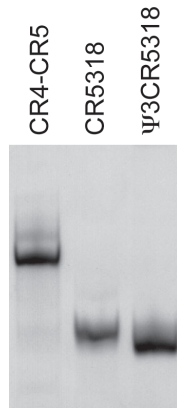


Figure S5. A 10 % non-denaturing polyacrylamide gel (19:1 acrylamide:bis-acrylamide) for the CR4-CR5 constructs. Full length CR4-CR5 (84 nt), CR5318 (57 nt), and Ψ 3CR5318 (57nt) all run predominantly as single bands indicating each folds into a single conformation.